Agriculture and Food

AIMS Agriculture and Food, 1(2): 124-143
DOI: 10.3934/agrfood.2016.2.124
Received 15 February 2016,
Accepted 7 April 2016,
Published 11 April 2016

http://www.aimspress.com/journal/agriculture

Research article

Soil losses in rainfed Mediterranean vineyards under climate change scenarios. The effects of drainage terraces.

María Concepción Ramos*

Department of Environment and Soil Science-Agrotecnio. University of Lleida. Rovira Roure 191, 25198 Lleida, Spain

* **Correspondence:** cramos@macs.udl.es; Tel: +341-973-702-092
Fax: +34-973-702-613.

Abstract: Most vines in the Mediterranean are cultivated on bare soils, due to the scarcity of water. In addition, most traditional soil conservation measures have been eliminated to facilitate the movement of machinery in the fields. In such conditions, high erosion rates are recorded. Given the predicted changes in precipitation and an increasing number of extreme events, an increase in erosion processes is expected. In this study, erosion processes under different climate change scenarios were evaluated as well as the effects of implementing drainage terraces in vineyards. Soil losses were simulated using the WEPP model. The results confirmed the relevance of extreme events on annual soil losses. The WEPP model gave satisfactory results in predicting runoff and soil losses, although the soil losses recorded after some extreme events were under-predicted. The model responded to changes in precipitation and because of that a decrease in precipitation gave rise to a decrease in soil losses. For the scenario in 2050, runoff volumes decreased between 19.1 and 50.1%, while erosion rates decreased between 34 and 56%. However, the expected increase in rainfall intensity may contribute to higher erosion rates than at present. The construction of drainage terraces, perpendicular to the maximum slope, 3 m wide and 30 m between terraces, may lead to an average decrease in soil losses of about 45%.

Keywords: climate change; drainage terraces; rainfed vineyards; soil erosion; soil water

1. Introduction

Soil erosion is a natural process that can be greatly accelerated by land use and climate changes, and is a major hazard to the long-term sustainability of agriculture and ecosystems. In the Mediterranean area, typical land uses such as olive trees, almond trees, orchards or vineyards are among those that incur higher rates of erosion. Among these land uses, vineyards are one in which greatest soil losses are recorded [1-4]. This may be due to a combination of rainfall and soil characteristics, as well as management. The Mediterranean climate is characterized by large variability in rainfall from to year to year, irregularly distributed throughout the year and with high intensity rainfall events, particularly in autumn. Some of these events are highly erosive [5], and usually one or two events every year are responsible for a high percentage of the annual soil losses. Most soils have loamy or loamy-sand textures, with an average percentage of coarse elements in the top horizon ranging between 10 and 20% and with relatively low organic matter content. In some cases soils are susceptible to sealing after some mm of rainfall. Thus, soils are susceptible to erosion processes.

In the Mediterranean, most vines are cultivated on bare soil, due to the scarcity of water. In addition, most traditional soil conservation measures were eliminated with the mechanization of almost all labors, mainly driven by the need to plant longer vine rows to facilitate the movement of machinery in the fields and to increase plant density. This required leveling and transforming land and reorganizing existing plots. The resulting cultivated soils, with altered profiles, lower organic matter content, poor structure and low infiltration capacities, are more susceptible to erosion processes [6,7]. Under these conditions, erosion losses in vineyards reach high values. Annual soil losses up to 25 Mg ha^{-1} have been recorded, most of which are recorded in a small number of events [8]. Even higher values have been recorded after some extreme events [9]. These soil losses not only represent the degradation of the soil due to higher losses, which surpass the soil loss tolerance, but additional nutrient losses [10] and increasing operational costs with negative impacts for vine growers [11].

The observed climate trends present additional threats for soil degradation with a potential increase of the magnitude of erosion processes. Different studies carried out in the Mediterranean region suggest that notable changes in seasonal precipitation regimes have occurred during the second half of the 20th century, which affected the main rainy seasons [12,13] with decreasing precipitation trends [14-17] and with an increase in extreme events in association with global warming [18-20]). The increase in the incidence of precipitation extremes may have an additional impact, due to greater water volumes being lost to runoff meaning less water infiltration and storage in the soil and an increase in the erosion processes [8,21]. Some predictions have been made for several different environments and according to dif2ferent scenarios, and also, using different models with different approaches and covering a range of spatial scales and time periods [22-25]. Among the most used models, WATEM-SEDEM [26]; PESERA [27]; SWAT [22]; EUROSEM [28]; WEPP [29]; R-USLE [30], or PSIAC [31] can be found. However, the expected increase in erosion rates was not always confirmed [32,33]. The results show that they seem to be affected by complex interactions of changes in rainfall distribution and intensity and in land use and management, which should be considered when climate change effects are considered [34-36].

In this study, soil losses under different rainfall distributions and climate change scenarios (2030 and 2050) in an area with a Mediterranean climate are analyzed. The effect of implementing drainage terraces in new vineyards to reduce soil losses is simulated for vineyards cultivated under rainfed conditions using WEPP.

2. Materials and Method

2.1. Area of study

The area of study is located in the Anoia region, about 40 km northwest of Barcelona (1°46′11″E, 41°31′52″N, 340 m.a.s.l.). This area is located in the Penedès Depression, between the Serralada Pre-litoral pre-coastal mountain range and the Mediterranean Sea in Northeastern Spain (Figure 1). The climate is Mediterranean with maritime influence, characterized by two wet periods (spring and autumn) separated by hot, dry summers. High intensity rainfall events are usually recorded in autumn [37]. The soils have developed on alluvial deposits from the Pleistocene Epoch, which are covered with a substratum of Miocene marls, sandstones and unconsolidated conglomerates. A high percentage of coarse elements of metamorphic origin is present in the soils. The evaluations were carried out at plot scale in one vineyard in which the soils, according to the soil map (1:25,000) of the Penedès region [38], are classified as *Typic Xerorthents* and *Fluventic Haploxerepts*. Sand contents ranged between 27.7 and 50%; silt content ranged between 37 and 47.2% and clay content ranged between 13 and 25.1%, while organic matter content ranged between 0.7 and 1.4%. The main land use is vines, which cover about 40% of the area [39].

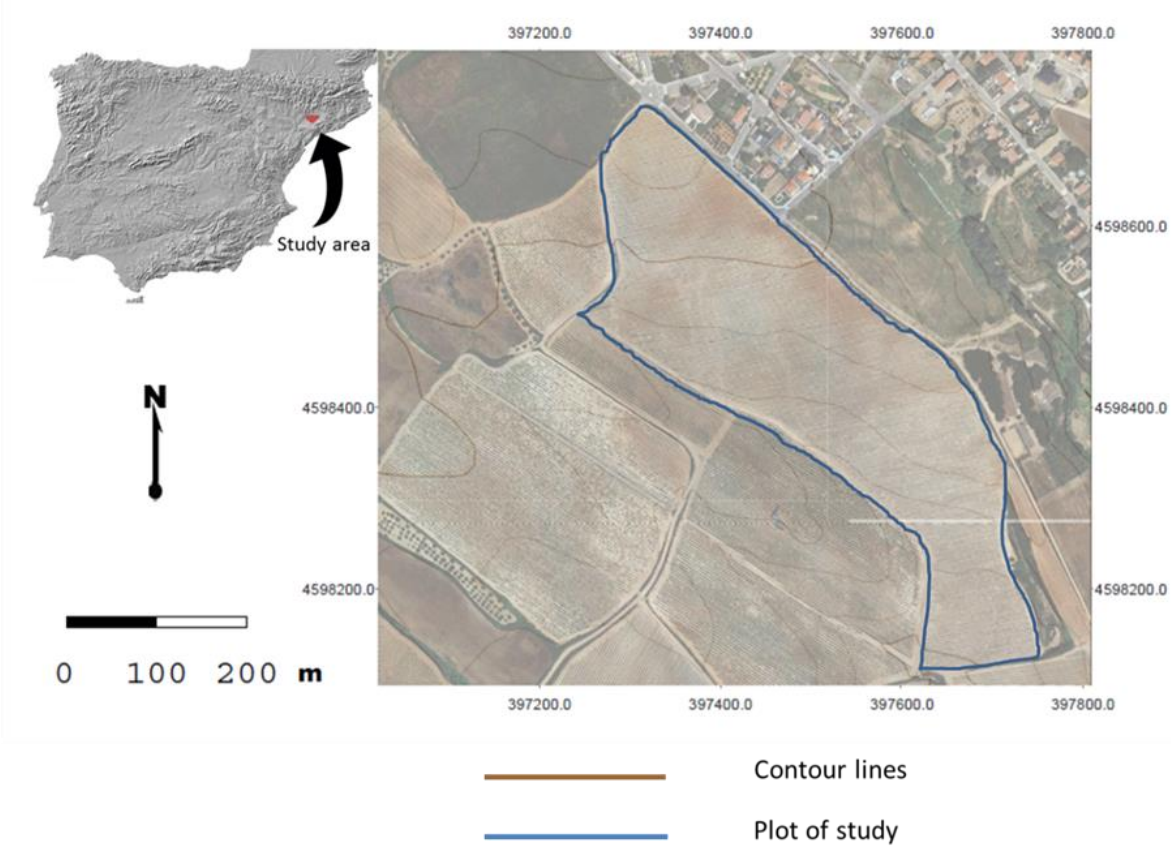

Figure 1. Location of the study area.

2.1.1. Field survey

The studied plot (Figure 1) was planted in 1990 and was levelled before vine plantation. It

produced significant disturbances to the original soil profile and created variability in soil properties within the plot. The plantation consists of trained vines with 3 m between rows and 3 m between plants, orientated NNE-WSW, on an average gradient of about 7%. The field study was carried out in 2010, 2011 and 2012, which had different amounts of rainfall and distribution. Within the plot, soil properties were evaluated at three locations (up (1), middle (2) and down slope (3)). pH, soil particle distribution [40], bulk density [41], organic carbon [42], water retention capacity at saturation, −33 and −1500 kPa (Richard Plates) were evaluated. The coarse element fraction was evaluated in an aliquot fraction of 2 kg, which was sieved using a 2 mm mesh. In addition, steady infiltration was evaluated using simulated rainfall. Plots, 0.30 m × 0.20 m were delimited in the field and subjected to 70 mm h^{-1} simulated rainfall composed of 2.5 mm diameter drops of deionized water falling freely from droppers 2.5 m above the soil surface. Runoff water was collected at 5-minute intervals for 50 minutes.

Soil characteristics of the soil surface at those locations are shown in Table 1. Most soils have a loamy-sandy or sandy texture, with the average percentage of coarse elements ranging from 20 to 30% in the top horizon. Organic matter content is relatively low (<1.4%). Water retention capacity at −33 kPa ranges between 16 and 22%, while at −1500 kPa the value ranges between 5.24 and 7.24%. Bulk density also varies within the plot, with an average value of about 1540 kg m^{-3}. Based on this average value and taking into account that tillage may produce a reduction in bulk density, the average bulk density after tillage considered in the model was 1500 kg m^{-3}.

Table 1. Soil characteristics of soil surface at three positions within the studied plot.

Area	Clay %	Silt %	Sand %	O.M. %	Bulk density kg m^{-3}	pH	FC (−33 kPa) %	PWP (−1500 kPa) %	Infiltration rates mm h^{-1}
1	8.5 ±4.6	22.9 ±4.6	68.6 ±8.8	1.18 ±0.37	1545 ±120	8.53	19.55	6.25	27
2	4.5 ±3.0	13.6 ±2.1	81.9 ±4.6	1.32 ±0.22	1670 ±55	8.55	16.11	5.27	28
3	5.0 ±2.3	17.9 ±3.9	77.1 ±6.0	1.37 ±0.21	1420 ±89	8.66	21.89	7.24	10.3

Soil depth ranges from 0.80 to 1.5 m. Soil water was monitored at four depths (10–30, 40–50, 50–70, 70–90 cm) in each plot every 15 days using Time Domain Reflectometry (TDR) IMKO tube-probes. The average soil water values for the profile were used to test the soil water simulated by the model. At the same positions, runoff samples were collected after the events that produced runoff using Gerlach collectors. Sediment concentrations in runoff were measured in each sample using an aliquot which was dried at 105 ºC and weighed. The results obtained were then used in conjunction with runoff water volumes to calculate soil losses for each runoff sampling point.

2.1.2. Climatic data

Climatic data were recorded at Els Hostalets de Pierola (long. 41.46°; lat. −1.81°; elev. a.l. 326 m), close to the study vineyard plot. This station belongs to METEOCAT (Institut Meteorologic de Catalunya). Hourly maximum, minimum and dew point temperature, precipitation, solar radiation, relative wind velocity and direction from the period 1996–2014 were recorded. Means and standard deviations of each variable were calculated. During the period of study additional rainfall data at 1

min intervals were collected at the plot. Years with different rainfall amount and distribution were identified and considered for further analysis. Temperature and precipitation changes in climate were simulated for 2030 and 2050 using the HadCM3 GCM predictions for the Representative Concentration Pathways (RCP) scenarios RCP8.5. Changes in solar radiation and relative humidity were taken for the prediction made for scenario A2. The data were downscaled to daily time step. The average monthly changes of these variables for each scenario are summarized in Table 2.

Table 2. Average monthly changes in temperature, humidity, wind velocity, and solar radiation for the 2030 and 2050 scenarios.

	Jan	Feb	Mar	Apr	May	Jun	Jul	Aug	Sep	Oct	Nov	Dec
2030												
T_{max} (ºC)	0.694	0.816	1.147	0.894	1.034	1.372	1.675	2.248	1.647	1.552	0.613	0.573
T_{min} (ºC)	0.639	0.630	0.769	0.643	0.863	1.028	1.290	1.868	1.347	1.517	0.674	0.388
SR (W/m^2)	0.129	0.076	7.606	4.600	−0.303	11.748	14.851	11.003	6.296	−0.354	0.321	0.170
P (%)	−3.64	−4.17	−15.92	−5.12	−9.10	−17.98	−25.08	−13.74	−0.40	24.95	6.38	−4.03
RH (fraction)	0.49	−0.56	−2.65	−2.37	−0.41	−1.75	−2.52	−2.21	−1.89	−0.36	−1.62	−1.30
WV (%)	−1.65	0.61	0.00	4.04	−1.70	1.83	1.80	−1.62	0.70	−0.75	2.87	2.65
2050												
T_{max} (ºC)	1.450	1.888	1.633	1.461	1.831	2.438	3.360	4.198	3.129	2.251	1.628	1.388
T_{min} (ºC)	1.215	1.719	1.455	1.054	1.363	1.832	2.366	2.982	2.499	2.157	1.705	1.326
SR (W/m^2)	−0.142	−1.047	5.286	8.094	6.182	10.937	22.325	20.637	12.504	1.366	0.442	−1.647
P (%)	1.86	3.18	−12.32	−17.37	−23.41	−23.65	−32.91	−31.91	−25.91	9.14	6.17	1.86
RH (fraction)	−0.75	−0.84	−2.86	−3.16	−2.32	−2.24	−4.13	−5.46	−4.18	−1.58	−1.70	−0.99
WV (%)	1.48	−0.58	3.08	1.34	1.69	0.49	−3.29	−4.20	−3.46	−0.63	−1.29	−1.30

2.2. Runoff and soil loss simulation: WEPP model

The hillslope version WEPP (v2012.8), which computes erosion along a single slope profile, was used in this study. The surface hydrology and water balance, subsurface hydrology, soils, plant growth, overland-flow hydraulics, and erosion components were considered. The description of the model was taken from Pieri et al. [43]. The surface hydrology and water balance routines use information on weather, vegetation and cultural practices. Infiltration in the model is computed by a Green-Ampt Mein-Larson equation [44] modified for unsteady rainfall [45]. Actual evapotranspiration (ET) is evaluated using a modified Ritchie's model [46], with reference potential ET estimated from the Penman-Monteith model [47]. Rainfall interception by canopy, surface depressional storage, soil water percolation, and subsurface lateral flow are also considered. Water partitioning between infiltration and runoff depends on hydraulic conductivity and saturation. The subsurface flow simulation is based on a mass continuity approach developed by Sloan and Moore [48]. The overland-flow is based on the approximate solutions to kinematic wave equations. The erosion component includes interrill and rill erosion and soil detachment by raindrop impact and subsequent sediment delivery as a function of the flow shear stress and transport capacity of concentrated flow. The plant-growth routines calculate biomass production for both crops and rangeland plants. The inputs for the model are described below.

2.2.1. Model input data

Table 3. Vegetation parameters and management inputs in the WEPP model for grape vine.

Initial conditions	Values	Plant growth and harvest parameters	Values
Bulk density after last tillage (g/cm^3)	1.5	Biomass energy ratio (kg/MJ)	30
Initial canopy cover (%)	10	Growing degree days to emergence (dgd)	30
Days since last harvest (days)	180	Growing degree days for growing season (gdd)	2000
Days since last tillage (days)	30	In-row plant spacing (m)	3
Initial interril cover (%)	10	Plant stem diameter at maturity (cm)	5
Initial residue cropping system	0	Harvest index (dry crop yield/ total above ground biomass) (%)	50
Cummulative rainfall since last tillage	200		
Initial ridge height since the last tillage (cm)	2	Canopy, LAI and Root Parameters	
Initial rill cover (%)	10	Canopy cover coefficient	14
Initial roughness after last tillage (cm)	1	Parameter value for canopy height equation	23
Rill spacing (m)	0	Maximum canopy height (m)	2
Rill width type	Temporary	Maximum leaf area index	6
Depth secondary tillage layer (cm)	35	Maximum root depth (m)	1.5
Depth primary tillage layer (cm)	20	Root to shoot ratio	0.3
Initial rill width (cm)	2	Maximum root mass for perennial crop (kg/m2)	0.6
Initial total dead root mass (kg/m^2)	0.5		
Initial total submerged residue mass (kg/m^2)	0.2		
Temperature and radiation parameters			
Base daily air temperature (ºC)	10		
Optimal temperature for plant growth (ºC)	25		
Maximum temperature that stops the growth (ºC)	35		
Critical freezing temperature (ºC)	−40		
Radiation extinction coefficient	0.65		
Management			S, Ch, C
Plant beginning	Apr 1st		
Tillage information			
Subsoil-chisel (S)	Jan 15th	Mean tillage depth (cm)	20, 20, 10
Chisel plow, rolling dick (Ch)	Feb 15th	Fraction of surface area disturbed (%)	100, 100, 95
	Apr 1st	Random roughness value after tillage (cm)	1.5, 1.5, 1.5
Cultivator (C)	May 20th	Ridge interval (cm)	7.5, 30, 75
	Jun 20th	Ridge height value after tillage (cm)	100, 5, 15
Harvest-Annual	Sep 10th		

Climate data: Daily maximum, minimum and dew point temperature, precipitation, solar radiation, relative wind velocity and direction from the period 1996–2014 were used. Breakpoint climate data series were used as inputs for the Water Erosion Prediction Project (WEPP), which were generated using the BPCDG2 software.

Soil characteristics: Soil properties such as pH, CEC, soil particle distribution (clay, silt, sand and rock fragment contents), organic matter content, bulk density, hydraulic conductivity, water retention capacity −33 and −1500 kPa were included. The soil water level measured in the field was used to parametrize the initial saturation level. Soil erosion was predicted for the different soil characteristics and then averaged for the plot.

Land management: Basic parameters related to grape vine were extracted from the WEPP database [49] and completed with information obtained from the literature [50,51] and own data derived from previous studies in the area. Land management and field-implemented tillage practices were modified according to the information given by the grape growers in the area. In the study plots, soil was bare most of the time with frequent tillage. The specific vegetation parameters for vines used by the model are shown in Table 3.

2.2.2. Model calibration and validation

The calibration of the model was carried out according to the procedure suggested by Alberts et al. [52] in the WEPP documentation. The model response to changes in drainage conditions and the parameters such as interrill erodibility, rill erodibility, critical shear and effective hydraulic conductivity were evaluated and explored on the outputs. These parameters were adjusted one by one starting with the average values recommended by the WEPP documentation [53]. For other parameters, information available from previous studies in the area and evaluations carried out in the field were considered. Calibration was then carried out by manually adjusting these parameters until reaching the best fit between simulated and measured soil loss. The soil water level measured in the field was used to parametrize the initial saturation level.

Calibration was carried out for the years 2010–2011 while 2012 was used for validation. Simulated runoff and soil losses were compared with the data obtained in the field survey. For each event the simulated runoff and soil loss integrated over time were compared with the average measured values. Model performance for both calibration and validation periods was evaluated following the criteria proposed by Moriasi et al. [54], based on three statistical methods: Nash-Sutcliffe efficiency (NSE; [55]), percent bias (PBIAS, %; [56]) and the ratio of the root mean square error to standard deviation (RSR) (Equations 1, 2 and 3).

$$NSE = 1 - \frac{\sum_{i=1}^{n}\left(Y_m - Y_s\right)^2}{\sum_{i=1}^{n}\left(Y_m - \bar{Y}\right)^2} \quad (1)$$

$$PBIAS = \frac{\sum_{i=1}^{n}\left(Y_m - Y_s\right)*100}{\sum_{i=1}^{n}\left(Y_m\right)} \quad (2)$$

$$RSR = \frac{\sqrt{\sum_{i=1}^{n}\left(Y_m - Y_s\right)^2}}{\sqrt{\sum_{i=1}^{n}\left(Y_m - \bar{Y}\right)^2}} \quad (3)$$

where Ym is the measured value and Ys is the simulated value with the model, and ($\bar{Y}$) is the mean of the measured values of each of the parameters analyzed. In order to analyze soil erosion under different climate scenarios two different rainfall distributions were considered. The simulations were based on two years with annual rainfall close to the average: one year with annual rainfall of 555.8 mm, in which rainfall was mainly concentrated in spring (41%) and autumn (34%) and another year with annual rainfall of 509 mm in which spring and autumn rainfall represented 37 and 43% of annual rainfall, respectively. The predicted changes for the climate change scenario and for different time periods were applied two both years in order to ascertain their effects on runoff and erosion rates. Additionally, increases of 10 and 20% were considered based on the trends observed in the area of study [5].

2.3. Simulation of the effect of drainage terraces on runoff and soil losses

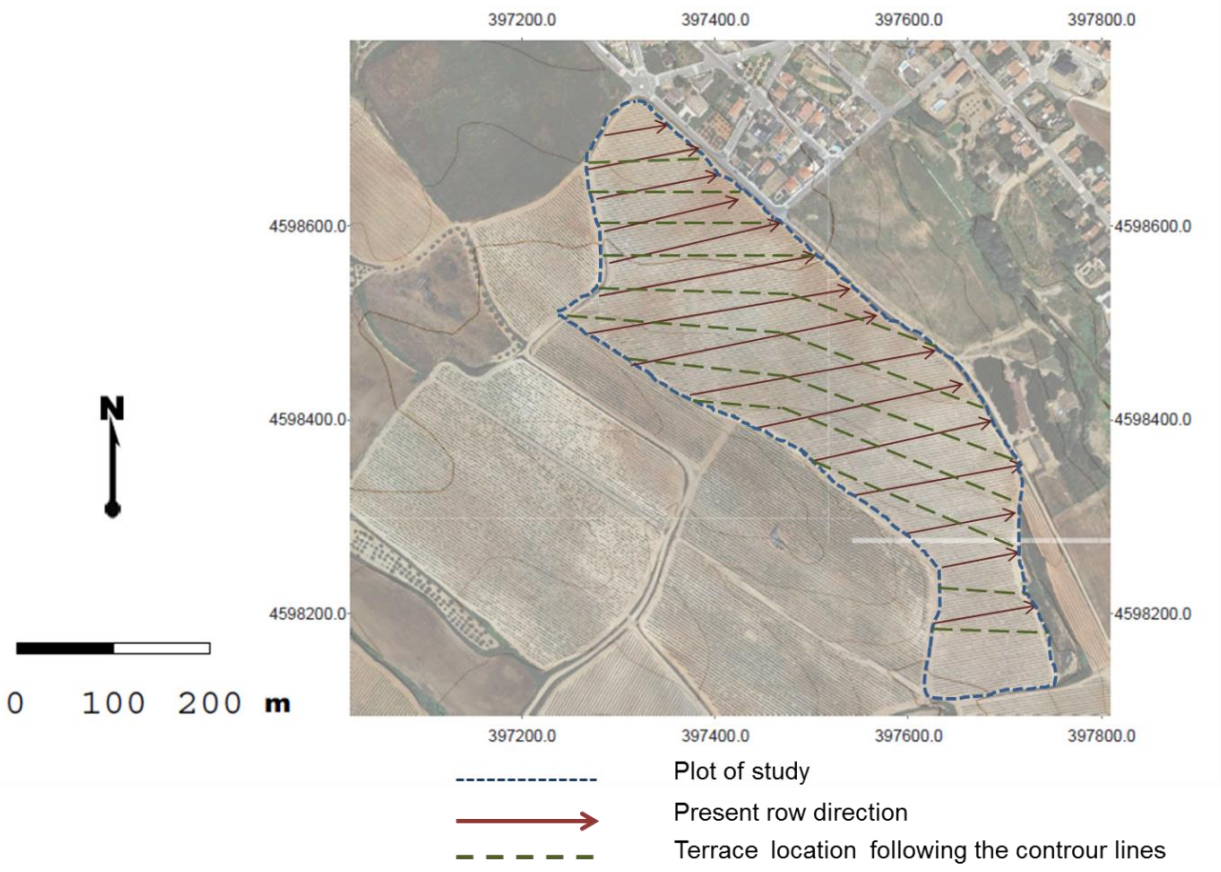

Figure 2. Present vine row direction and optimum direction of the drainage terraces in the plot of study.

Drainage terraces (locally known as “rases”) were soil conservation measures used in the past in

this viticulture area. However, in the new vineyard planted for management with machinery these practices were eliminated. Their construction does not reduce soil cultivation surface as they can be constructed between vine rows. In order to find a suitable design for the area, according to the slope of the terrain and the rainfall characteristics, a previous study carried out in the area [57], based on the limits of soil loss tolerance, was taken into consideration. Based on the average land slope, the optimum horizontal distance between terraces should be about 28 m. Given the plantation pattern, with 3 m between rows, a separation between terraces of 30 m was established while the width of the terraces was 3 m. The slope was modified according to that design. Other parameters of terrace design, such as the shape and the capacity of the terraces to carry the peak flow rate should be defined when constructing them, but these parameters are not considered as input data in the model. The terraces must be constructed across the slope on a contour. In the study plot, the vine rows are not planted following this logic in all plot. Figure 2 shows the present direction of the vine rows and the proposed location of the terraces in the vineyard studied. Thus the construction of the terraces could be not constructed at relatively low cost at present but it should be considered in a new vineyard replanting.

3. Results

3.1. Runoff and soil losses in the years analyzed

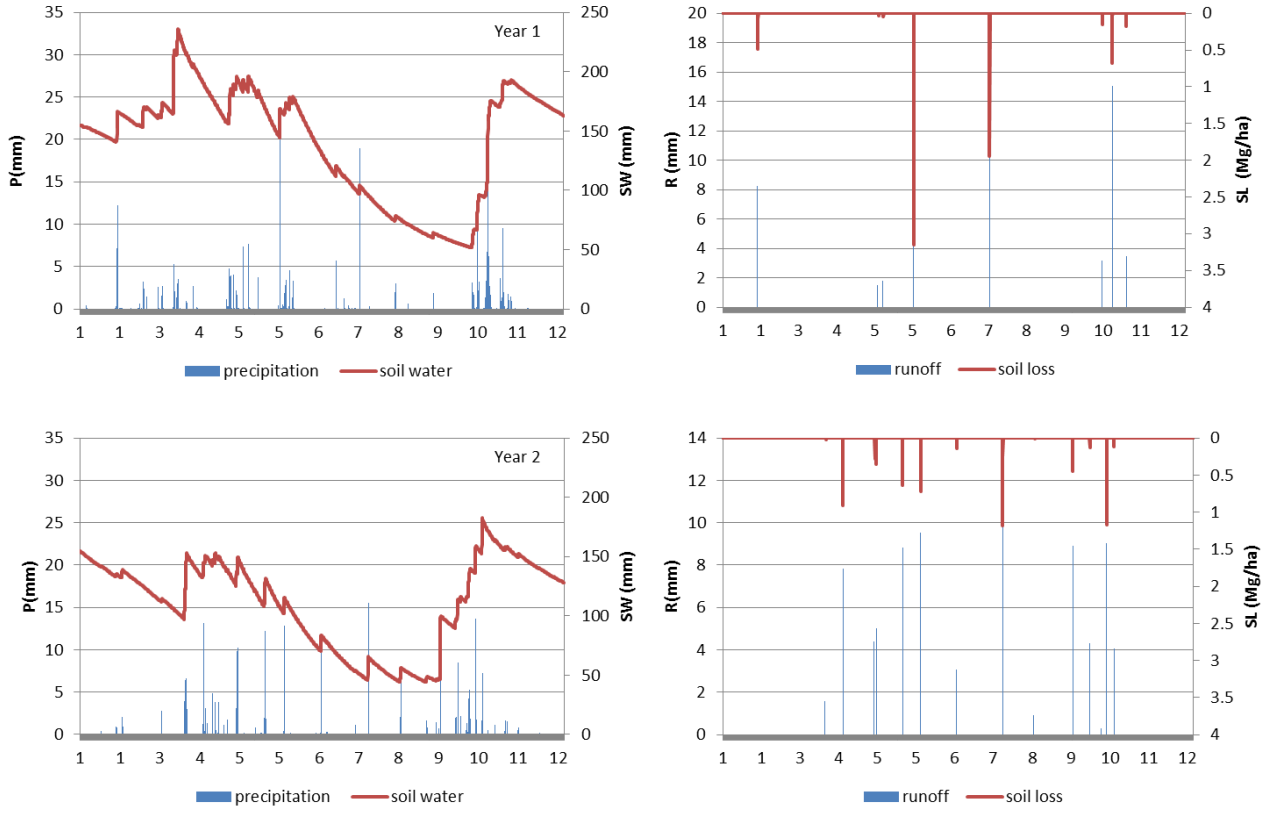

Figure 3. Precipitation, soil moisture, runoff and soil losses simulated for the selected years.

Figure 3 shows the precipitation and average soil moisture recorded during the years analyzed.

Within the period analyzed rainfall varied between 509 and 555.8 mm. In 2010, ten events produced runoff, which accounted for about 26% of rainfall. Most runoff was recorded in summer and in autumn. In one event in summer recorded 75% of rainfall run off. In 2011, 21 events with more than 9 mm were recorded, but only seven of them produced runoff and erosion. The rainfall recorded in those events represented 41% of annual rainfall and 25% of rainfall run off. In 2012, rainfall was mainly distributed in spring and autumn and 20 events produced runoff. Runoff represented about 22% of annual rainfall distributed in all seasons of the year. Annual soil losses ranged between 6.8 Mg ha^{-1} in 2012 and about 10 Mg ha^{-1} in 2011. Most soil losses were recorded in a small number of events. During the years analyzed, the highest erosive event was recorded in the summer of 2010, in which 50% of annual soil losses were recorded. In 2011 soil losses were mainly recorded in spring and summer. In 2012, there were no extremely erosive events. Soil losses were distributed throughout the year although the highest soil losses were recorded in spring (66% of annual erosion).

3.2. Runoff and soil losses simulated using WEPP: under present conditions and climate change scenarios

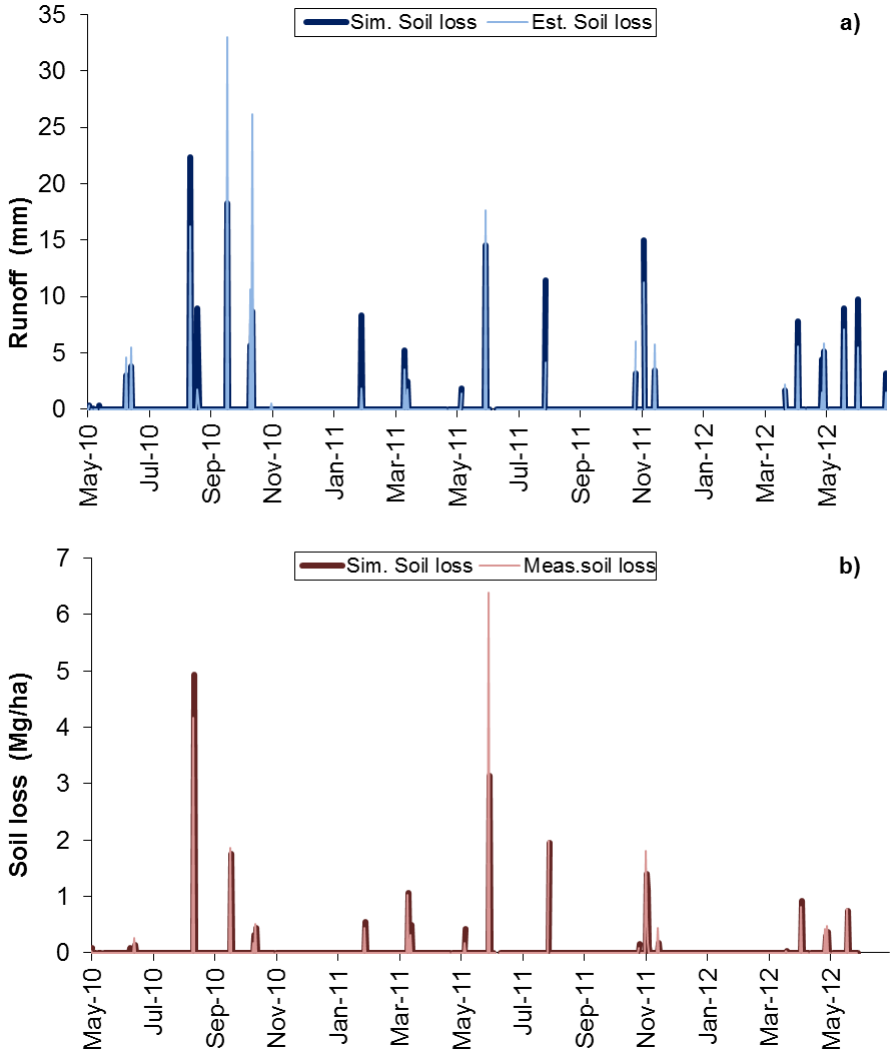

Figure 4. Runoff (a) and soil loss (b) measured and simulated with WEPP for the erosive events recorded during the calibration and validation periods.

Figure 4 shows the comparison between runoff and soil loss measured and simulated with WEPP used for the erosive events recorded during the calibration and validation periods. The main rainfall events were simulated. However, the simulated runoff rates were smaller than the values measured in those events in which rainfall was concentrated in a limited number of hours. For soil erosion, the model simulated detachment but there was no deposition in any case. The simulated values were slightly smaller than the values measured for most cases, with greater differences in the extreme events. Table 4 shows the statistics used to analyze the performance of the model for both periods (calibration and validation). According to the criteria proposed by Moriasi et al. [54], the performance of the model may be considered good for runoff and sediment yield based on NSE, RSR and PBIAS (NSE > 0.65, RSR > 0.60 and PBIAS < 15% for runoff and 25% for sediment) during the calibration period and satisfactory during the validation period (NSE > 0.65, RSR < 0.70 and PBIAS < 25% for runoff and 6.75% for sediment).

After validation of the model, runoff and erosion rates were simulated for the years 2011 and 2013, which were the years for which the climate change analyses were analyzed. The recorded rainfall and the simulated runoff, soil water and soil losses for each year are presented in Figure 3. It can be observed how rainfall amount and distribution have a clear effect not only on soil water but also on runoff and erosion rates. In year 1, total rainfall was slightly higher than in year 2, but the most relevant aspect was its distribution. In year 1 it was more concentrated in spring and autumn while in year 2 it was more homogeneously distributed in spring, summer and autumn and the contribution of single events was smaller. The contribution of each event to annual soil losses was smaller in year 2 than in year 1. The annual and seasonal results are summarized in Tables 5 and 6.

The results of the simulations for the different climate scenarios (with additional increases of 10 and 20% for 2030 and 2050) are presented in the same tables. For both rainfall distributions (represented in the two analyzed years) the reduction in rainfall amount and the increase in temperature gave rise to a decrease in runoff and erosion rates. However, the effect of rainfall intensity increase was also evident, which is in agreement with the expected increase of erosion rates under the climate change scenario.

3.3. Simulated soil losses under present conditions and with drainage terraces

The predicted soil losses with and without terraces, for the analyzed scenarios (two different rainfall distributions and increasing intensities, for different time periods) are shown in Table 7. The average predicted reduction in soil losses associated with the construction of terraces ranged between 31 and 59%, with an average of 45%. The reduction in soil losses was mainly due to deposition within the fields, while in the situation without soil conservation measured, the simulated deposition was null.

Table 4. Statistics used to evaluate the performance of the model for runoff and soil losses.

	Calibration			Validation		
	RSR	NSE	PBIAS	RSR	NSE	PBIAS
Runoff	0.858	0.711	−9.582	0.532	0.786	14.733
Soil losses	0.521	0.828	−25.135	0.810	0.718	−6.667

Table 5. Simulated rainfall, runoff, infiltration, evaporation, deep percolation, soil water and erosion rates for rainfall conditions of year 1 (2011) under each scenario (2030 and 2050 and 10% (+i10) and 20% (+i20) increasing intensity).

Year-scenario	Period	Rainfall (mm)	Infilt. (mm)	Evap. (mm)	Deep percol. (mm)	Runoff (mm)	Soil water (mm)	Soil loss (Mg ha^{-1})
Year 1-present	Annual	555.10	493.99	438.44	49.21	59.24	140.91	9.55
	Winter	60.70	52.17	58.22	7.36	8.28	161.67	0.75
	Spring	232.50	213.82	175.70	33.35	17.87	182.92	4.30
	Summer	71.20	59.25	152.00	2.37	11.43	119.29	2.59
	Autumn	190.70	168.75	52.54	6.14	21.66	99.78	1.91
Year 1-2030	Annual	536.31	479.41	429.21	40.99	56.90	137.73	7.94
	Winter	58.74	51.28	59.23	8.11	7.46	162.53	0.64
	Spring	211.84	196.96	172.56	23.59	14.88	177.45	3.37
	Summer	59.15	51.65	145.40	1.47	7.50	112.37	1.12
	Autumn	206.57	179.53	52.01	7.83	27.05	98.72	2.82
Year 1-2030+i10	Annual	536.31	465.25	423.82	36.13	71.86	135.72	9.62
	Winter	58.74	48.17	58.31	6.64	8.71	160.04	0.75
	Spring	211.84	196.15	172.00	22.59	18.53	176.75	4.34
	Summer	59.15	49.18	143.16	1.35	7.45	110.67	2.62
	Autumn	206.57	171.74	50.35	5.56	37.17	95.50	1.91
Year 1-2030+i20	Annual	536.31	431.29	409.42	25.80	78.40	130.84	11.73
	Winter	58.74	45.83	56.89	4.64	9.29	155.70	0.84
	Spring	211.84	184.91	166.76	17.39	21.70	171.75	4.83
	Summer	59.15	42.79	139.28	1.04	10.42	107.65	1.10
	Autumn	206.57	157.77	46.49	2.74	36.98	88.35	4.95
Year 1-2050	Annual	502.60	453.20	414.20	34.00	47.92	131.80	6.28
	Winter	62.20	53.10	60.50	6.90	8.85	160.70	0.73
	Spring	188.70	179.30	169.90	21.00	8.68	173.40	1.75
	Summer	48.80	44.50	135.20	0.70	3.92	102.20	0.31
	Autumn	202.90	176.30	48.60	5.50	26.47	91.20	3.49
Year 1-2050+i10	Annual	502.60	438.27	406.56	31.12	62.02	129.50	8.37
	Winter	62.20	52.51	59.61	5.72	9.99	158.30	0.98
	Spring	188.70	175.00	168.99	20.96	10.84	172.70	2.33
	Summer	48.80	41.43	130.99	0.51	4.55	99.10	0.41
	Autumn	202.90	169.34	46.96	3.93	36.64	88.10	4.65
Year 1-2050+i20	Annual	502.60	431.30	409.40	25.80	78.40	128.37	10.38
	Winter	62.20	45.80	56.90	4.60	9.29	157.20	0.77
	Spring	188.70	184.90	166.80	17.40	21.70	172.35	4.34
	Summer	48.80	42.80	139.30	1.00	10.42	97.77	1.61
	Autumn	202.90	157.80	46.50	2.70	36.98	86.66	3.67

Table 6. Simulated rainfall, runoff, infiltration, evaporation, deep percolation, soil water and erosion rates for rainfall conditions of year 2 (2013) under each scenario (2030 and 2050, and 10% (+i10) and 20% (+i20) increasing intensity).

Year-scenario	Period	Rain (mm)	Infilt. (mm)	Evap. (mm)	Dep Percol. (mm)	Runoff (mm)	Soil water (mm)	Soil loss (Mg ha^{-1})
Year 2-present	Annual	530.5	435.4	412.4	44.40	92.60	117.80	7.28
	Winter	14.5	12.3	62	12.8	0	136	0.00
	Spring	195	165	160.1	9.4	29	127.8	2.29
	Summer	93	63.1	114.6	0.2	27	70.1	2.39
	Autumn	228	195	75.7	22	36.6	110.2	2.59
Year 2-2020	Annual	510.7	428.3	407.8	47.7	81.12	109.4	6.67
	Winter	11.8	11.7	62.9	12.5	0.00	136.4	0.00
	Spring	176.6	153.0	157.0	6.6	22.93	123.9	1.80
	Summer	77.6	59.8	111.1	0.1	17.61	66.9	1.31
	Autumn	244.7	203.9	76.8	28.4	40.58	110.8	3.56
Year 2-2020+i10	Annual	510.3	406.0	397.0	38.0	103.26	107.0	9.52
	Winter	11.3	11.2	62.6	11.9	0.00	135.6	0.00
	Spring	176.3	146.6	154.8	6.0	29.06	122.5	2.60
	Summer	78.5	55.4	106.1	0.1	23.00	63.9	1.97
	Autumn	244.2	192.8	73.5	20.1	51.20	106.5	4.94
Year 2-2020+i20	Annual	509.7	382.9	385.0	29.0	125.79	104.2	12.95
	Winter	11.8	11.7	62.3	11.1	0.00	134.6	0.00
	Spring	170.9	135.1	149.9	4.5	35.31	119.1	3.54
	Summer	83.0	54.6	102.7	0.1	28.24	61.8	2.75
	Autumn	244.0	181.6	70.2	13.4	62.23	101.9	6.65
Year 2-2050	Annual	437.2	390.7	390.4	31.1	45.41	103.6	3.14
	Winter	12.0	11.9	64.1	11.2	0.00	134.6	0.00
	Spring	154.1	140.2	152.4	4.7	13.26	119.4	0.71
	Summer	59.6	52.6	104.4	0.1	6.87	61.4	0.32
	Autumn	211.5	186.1	69.5	15.2	25.28	99.6	2.10
Year 2-2050+i10	Annual	437.0	437.0	437.0	437.0	61.49	101.7	4.63
	Winter	11.5	11.5	11.5	11.5	0.00	133.6	0.00
	Spring	154.3	154.3	154.3	154.3	18.05	118.3	1.14
	Summer	60.4	60.4	60.4	60.4	9.93	59.5	0.55
	Autumn	210.8	210.8	210.8	210.8	33.51	96.1	2.95
Year 2-2050+i20	Annual	436.1	356.4	372.3	20.4	78.87	99.3	6.48
	Winter	12.0	11.9	63.2	9.8	0.00	132.4	0.00
	Spring	149.5	126.2	146.5	3.5	22.84	115.4	1.63
	Summer	64.0	50.4	98.1	0.0	13.46	57.7	0.84
	Autumn	210.6	167.9	64.5	7.0	42.57	92.3	4.02

Table 7. Comparison of soil losses with and without terraces in the analyzed scenarios (SL: soil losses; D: deposition)

Year/scenario	Without terraces	With terraces		Year/scenario	Without terraces	With terraces	
Year 1	SL	SL	D (%)	Year 2	SL	SL	D (%)
Year 1-present	6.78	2.78	30	Year 2-present	9.55	3.92	39
Year 1-2020	6.67	4.59	33	Year 2-2020	7.94	5.46	31
Year 1-2020_i10	9.51	6.58	39	Year 2-2020_i10	8.8	6.08	30
Year 1-2020_i20	12.95	8.83	32	Year 2-2020_i20	11.73	7.01	40
Year 1-2050	3.14	2.16	40	Year 2-2050	5.35	2.72	41
Year 1-2050_i10	4.63	2.35	22	Year 2-2050_i10	8.37	5.76	32
Year 1-2050_i20	6.48	2.66	21	Year 2-2050_i20	10.38	4.26	35

4. Discussion

Soil losses recorded during the analyzed period were of the same order of magnitude as those observed in the area in previous years [8,10]. Annual soil losses were mainly recorded in a small number of events, with total values that exceed the soil loss tolerance rate established for Europe (0.3 to 1.4 Mg ha^{-1} yr^{-1}) [58] and higher permissible values established for arable lands, which range between 2.2 and 12 Mg ha^{-1} yr^{-1} [59,60]. The results confirmed the importance of extreme events on runoff generation and on annual erosion rates. For example, threshold values are considered permissible.

The use of the Water Erosion Prediction Project (WEPP) gave satisfactory results to predict average annual soil losses. However, the model did not simulate all erosion events well, in particular those that generated very little runoff, and those that contributed more to total annual erosion. The former did not contribute significantly to total runoff and erosion. However, the most erosive events, which were usually concentrated in a short time interval and generated high runoff rates, were under-predicted. Nevertheless, the statistics used to analyze the performance of the model confirmed that the results could be considered satisfactory, taking into account that the calibration was carried out using daily data. Licciardello et al. [61] pointed out some limitations of the model when dry and wet conditions were considered together, and this could also be the reason for the lack of goodness of fit of all events. It can be observed that the statistics showed better fit for the validation than for the calibration period, which may seem strange. This result was attributed to the fact that during the validation period no extreme events were recorded. Despite these limitations, the model may be useful to compare the response regarding soil losses under different rainfall distributions and those that may be produced under different climate change scenarios.

The simulated trends in precipitation associated with climate change for the study area showed a decrease in rainfall for the coming decades, with a greater decrease for 2050 than for 2030. However, due to the different trends in spring and autumn, the two main rainfall periods in the area of study, the effect may be different from year to year. For the years analyzed, spring rainfall decreased while autumn rainfall increased. The simulation of the erosion rates responded to the changes in runoff, which were affected by less water availability due to temperature increase. For the 2030 scenario, runoff volumes decreased between 4 and 8%, while erosion rates decreased 2 and 16% respectively. For the 2050 scenario, however, the differences in runoff between years were greater. Runoff rates decreased between 19.1 and 50.1% in the 2050 scenario, while erosion rates decreased between 34

and 56%. Despite the expected increase in erosion rates with climate change, for both rainfall distributions the simulation showed a decrease in soil losses. Similar results have also been indicated by other researches [33,34]. These authors simulated changes in erosion rates of similar magnitude for Greece and for Ireland under climate change scenario A. This means that additional factors may condition soil losses that were not included in the simulation. In this respect, some studies indicate that although changes in soil erosion are driven by changes in rainfall, they may be affected by complex interactions including changes in rainfall distribution and intensity and in land use and management, which should be considered when the effects of climate change are considered [35-37]. In this respect Routschek et al. [62] indicate that the impacts of land use, soil management and soil properties on soil erosion by water are greater than the effects of changing precipitation patterns. In the study area, vine cultivation has been the main land use for centuries and at present it is a strong economic motor. Management practices have changed during recent decades, but there is no perspective of change in the midterm to a different land use or to dedicate the land to other activities. The main changes suffered in the area, associated with labor mechanization, has implied an increase of soil degradation and soil losses [7,63], and for this reason knowledge of additional potential effects is needed in order to establish new control measures.

One of the main changes in precipitation associated with climate change is the increasing strength and erosivity of rainfall events [64-66]. Evidence recorded in the area in different observatories during recent decades shows an increase in the maximum intensity of erosive events. The increase varied between observatories between about 12 and 20% [5]. The increase in rainfall erosivity has also been confirmed in other areas of Spain [67] in which erosion processes seem to increase, and also in other areas around the world [68-70]. In this respect, Shiono et al. [68] indicated an expected increase of 20% in the R-values compared with those in the recent past and predicted average erosion rates greater than 20% based just on the effects of the rainfall erosivity factor.

The simulations carried out in this study with increasing rainfall intensities, for the different scenarios confirmed the effect of intensity on soil erosion with significant increases in erosion rates. The results showed that the erosion rates for the 2030 scenario, may be up to 21.8% higher than at present considering an increase of 10% in rainfall intensity and up to 47% higher when rainfall intensity increased by 20%, for one of the rainfall distributions. For the second rainfall distribution, soil losses may be up to 46 and 95%, respectively for an increase of 10 and 20% in rainfall intensity. For the 2050 scenario, the increase of soil erosion rates could reach 100% in relation to the predicted values without rainfall intensity change. Despite the decrease in precipitation, erosion rates may increase due to the effect of the extreme events. Under the two analyzed rainfall distributions, the results of the simulation reached higher annual soil losses, than the soil loss tolerance. Thus, under the hypothesis of an increase of these situations associated with climate change, the high erosion rates point out the need for establishing some soil conservation measures.

The simulation of the soil terrace effect on soil losses confirmed its benefits. For the existing vine plantation pattern and the slope of the terrain, the construction of drainage terraces, 3 m width and spaced 30 m, i.e. every 10 vine rows, would reduce soil losses by about 45%, on average. The deposition simulated with the model was in agreement with observations carried out in the same area, where terraces were already constructed [11]. The function of the terraces was not only to evacuate the excess of runoff but to retain some of the sediments produced along the slope and prevent their removal from the field. The lowest reductions were observed in the driest situations and with the lowest erosion rates. The results of the simulation, regarding the reduction of soil losses, were in

agreement with previous simulations make at catchment scale using SWAT [71] and with those simulated or observed by other authors. Yang et al. [72] indicated a sediment yield reduction of about 56% when applying flow diversion terraces separated uniformly 60 m on slopes ranging between 3 and 8%. Even higher reductions in soil losses have been simulated. Thus Mwangui et al. [73] indicated that the introduction of parallel terraces reduced sediment losses by 85% and decreased surface runoff by 22%. Even higher reductions were found when contour planting is associated with terracing [74]. However, the effect of terraces may depend on the actual design of the terrace [75].

5. Conclusion

The results confirmed the difficulties for obtaining predictions for soil erosion processes due to the high variability of rainfall recorded in Mediterranean conditions as well as the contributions of extreme events to annual soil losses. Soil losses simulated under the predicted trends in precipitation and temperature may give rise to higher erosion than at present for certain rainfall distributions when increasing rainfall intensity is considered. A 10% increase in rainfall may result in soil losses up to 40% higher. Under these scenarios, there is a need to implement some soil conservation measures to reduce soil losses. The construction of drainage terraces, perpendicularly to the maximum slope, 3 m in width and separated 30 m between terraces may reduce soil losses significantly (up to about 45%).

Acknowledgments

This work is part of research project AGL2009-08353 which was funded by the Spanish Ministry of Science and Innovation. I would like to thank the Castell d'Age winery for their support for allowing us to carry out the field experiments on their property.

This research article has received a grant for its linguistic revision from the Language Institute of the University of Lleida (2016 call)

Conflict of interest

Author declare no conflicts of interest in this paper.

References

1. Tropeano D (1984) Rate of soil erosion processes on vineyards in Central Piedmont (NW Italy). *Earth Surf Process Landforms* 9: 253–266.
2. Wainwright J (1996) Infiltration, runoff and erosion characteristics of agricultural land in extreme storm events, SE France. *Catena* 26: 27–47.
3. Wicherek S (1991) Viticulture and soil erosion in the North of Parisian Basin. Example: The mid Aisne region. *Zeitschrift Für Geomorphol* 83: 115–126.
4. Kosmas C, Danalatos N, Cammeraat LH, et al. (1997) The effect of land use on runoff and soil erosion rates under Mediterranean conditions. *Catena* 29: 45–59.
5. Ramos MC, Durán B (2014) Assessment of rainfall erosivity and its spatial and temporal variabilities: Case study of the Penedès area (NE Spain). *Catena* 123: 135–147.

6. Ramos MC, Martínez-Casasnovas JA (2006) Impact of land levelling on soil moisture and runoff variability in vineyards under different rainfall distributions in a Mediterranean climate and its influence on crop productivity. *J Hydrol* 321: 131–146.
7. Ramos MC, Martínez-Casasnovas JA (2010) Soil water balance in rainfed vineyards of the Penedès region (Northeastern Spain) affected by rainfall characteristics and land levelling: influence on grape yield. *Plant Soil* 333: 375–389.
8. Ramos MC, Martínez-Casasnovas JA (2009) Impacts of annual precipitation extremes on soil and nutrient losses in vineyards of NE Spain. *Hydrol Process* 23: 224–235.
9. Martínez-Casasnovas J, Ramos M, Ribes-Dasi M (2002) Soil erosion caused by extreme rainfall events: mapping and quantification in agricultural plots from very detailed digital elevation models. *Geoderma* 105: 125–140.
10. Ramos MC, Martínez-Casasnovas JA (2006) Nutrient losses by runoff in vineyards of the Mediterranean Alt Penedès region (NE Spain). *Agric Ecosyst Environ* 113: 356–363.
11. Martínez-Casasnovas JA, Ramos MC (2006) The cost of soil erosion in vineyard fields in the Penedès–Anoia Region (NE Spain). *Catena* 68: 194–199.
12. de Luis M, Brunetti M, Gonzalez-Hidalgo JC, et al. (2010) Changes in seasonal precipitation in the Iberian Peninsula during 1946–2005. *Glob Planet Change* 74: 27–33.
13. Ramos MC, Balasch JC, Martínez-Casasnovas JA (2012) Seasonal temperature and precipitation variability during the last 60 years in a Mediterranean climate area of Northeastern Spain: a multivariate analysis. *Theor Appl Climatol* 110: 35–53.
14. Goubanova K, Li L (2007) Extremes in temperature and precipitation around the Mediterranean basin in an ensemble of future climate scenario simulations. *Glob Planet Change* 57: 27–42.
15. Bartolini G, Grifoni D, Torrigiani T, et al. (2014): Precipitation changes from two long-term hourly datasets in Tuscany, Italy. *Int J Climatol* 34: 3977–3985.
16. Nunes AN, Lourenço L (2015) Precipitation variability in Portugal from 1960 to 2011. *J Geogr Sci* 25: 784–800.
17. Tošić I, Zorn M, Ortar J, et al. (2016) Annual and seasonal variability of precipitation and temperatures in Slovenia from 1961 to 2011. *Atmos Res* 168: 220–233.
18. Easterling DR, Karl TR, Gallo KP, et al. (2000) Observed climate variability and change of relevance to the biosphere. *J Geophys Res Atmos* 105: 20101–20114.
19. Klein Tank AMG, Können GP (2003) Trends in Indices of Daily Temperature and Precipitation Extremes in Europe, 1946–99. *J Clim* 16: 3665–3680.
20. Kharin VV, Zwiers FW, Zhang X, et al. (2007) Changes in Temperature and Precipitation Extremes in the IPCC Ensemble of Global Coupled Model Simulations. *J Clim* 20: 1419–1444.
21. Favis-Mortlock DT, Boardman J (1995) Nonlinear responses of soil erosion to climate change: a modelling study on the UK South Downs. *Catena* 25: 365-387.
22. Nearing MA, Jetten V, Baffaut C, et al. (2005) Modeling response of soil erosion and flow to changes in precipitation and cover. *Catena* 61: 131-154
23. Mullan DJ, Favis-Mortlock DT, Fealy R (2011) Modelling the impacts of climate change on future rates of soil erosion: Addressing key limitations. In: ASABE - International Symposium on Erosion and Landscape Evolution 2011. pp 486–494.
24. Segura C, Sun G, McNulty S, Zhang Y (2014) Potential impacts of climate change on soil erosion vulnerability across the conterminous United States. *J Soil Water Conserv* 69: 171–181.

25. Cilek A, Berberoglu S, Kirkby M, et al. (2015) Erosion Modelling In A Mediterranean Subcatchment Under Climate Change Scenarios Using Pan-European Soil Erosion Risk Assessment (PESERA). ISPRS - Int Arch Photogramm Remote Sens Spat Inf Sci XL-7/W3: 359–365.
26. Haregeweyn N, Poesen J, Verstraeten G, et al. (2013) Assessing the performance of a spatially distributed soil erosion and sediment delivery model (WATEM/SEDEM) in northern Ethiopia. *Land Degrad Dev* 24: 188–204.
27. Kirkby MJ, Jones RJA, Irvine B, et al. (2004) Pan-European soil erosion risk assessment: the PESERA Map, Version 1 October 2003. Explanation of Special Publication Ispra 2004 No.73 (S.P.I.04.73). European Soil Bureau Research Report No.16, EUR 21176, 18pp.
28. Morgan RPC, Quinton JN, Smith RE, et al. (1998) The European Soil Erosion Model (EUROSEM): a dynamic approach for predicting sediment transport from fields and small catchments. *Earth Surf Process Landforms* 23: 527–544.
29. Laflen JM, Elliot WJ, Flanagan DC, et al. (1997) WEPP-predicting water erosion using a process-based model. *J Soil Water Conserv* 52: 96–102.
30. Renard KG, Foster GR, Weesies GA, et al. (1997) Predicting soil erosion by water: A guide to conservation planning with the revised universal soil loss equation (RUSLE). Handb. No. 703, Washington, DC US Dep. Agric.
31. de Vente J, Poesen J, Verstraeten G (2005) The application of semi-quantitative methods and reservoir sedimentation rates for the prediction of basin sediment yield in Spain. *J Hydrol* 305: 63–86.
32. Nerantzaki SD, Giannakis G V, Efstathiou D, et al. (2015) Modeling suspended sediment transport and assessing the impacts of climate change in a karstic Mediterranean watershed. *Sci Total Environ* 538: 288–297.
33. Mullan D (2013) Soil erosion under the impacts of future climate change: Assessing the statistical significance of future changes and the potential on-site and off-site problems. *Catena* 109: 234–246.
34. Mullan D, Favis-Mortlock D, Fealy R (2012) Addressing key limitations associated with modelling soil erosion under the impacts of future climate change. *Agric For Meteorol* 156: 18–30.
35. Orwin KH, Stevenson BA, Smaill SJ, et al. (2015) Effects of climate change on the delivery of soil-mediated ecosystem services within the primary sector in temperate ecosystems: a review and New Zealand case study. *Glob Chang Biol* 21: 2844–2860.
36. Simonneaux V, Cheggour A, Deschamps C, et al. (2015) Land use and climate change effects on soil erosion in a semi-arid mountainous watershed (High Atlas, Morocco). *J Arid Environ* 122: 64–75.
37. Ramos MC (2001) Rainfall distribution patterns and their change over time in a Mediterranean area. *Theor Appl Climatol* 69: 163–170.
38. DAR (2008) Mapa de Sòls (1: 25.000) de l'àmbit geogràfic de la Denominació d'Origen Penedès. Departament d'Agricultura, Alimentació i Acció Rural, Generalitat de Catalunya, Vilafranca del Penedès-Lleida.
39. IDESCAT. Anuario estadístico de Cataluña. Agricultura Ganadería y Pesca. 2013. Available from: http: //idescat.cat/pub/aec/es.

40. Gee GW, Bauder JW (1986) Particle-size Analysis. P. 383 – 411. In A.L. Page (ed.). *Methods of soil analysis*, Part1, Physical and mineralogical methods. Second Edition, Agronomy Monograph 9, American Society of Agronomy, Madison, WI.
41. Cresswell HP and Hamilton (2002) Particle Size Analysis. In: *Soil Physical Measurement and Interpretation For Land Evaluation*. (Eds. NJ McKenzie, HP Cresswell and KJ Coughlan) CSIRO Publishing: Collingwood, Victoria, 224-239.
42. Allison LE (1965) Organic Carbon. In: *Methods of Soil Analysis*, Black, C.A. (Ed.). American Society of Agronomy, USA, 1367-1378.
43. Pieri L, Bittelli M, Wu JQ, et al. (2007) Using the Water Erosion Prediction Project (WEPP) model to simulate field-observed runoff and erosion in the Apennines mountain range, Italy. *J Hydrol* 336: 84–97.
44. Mein RG, Larson CL (1973) Modelling infiltration during a steady rain. *Water Resour Res* 9: 384-394
45. Chu ST (1978) Infiltration during an unsteady rain. *Water Resour Res* 14: 461–466.
46. Ritchie JT (1972) Model for predicting evaporation from a row crop with incomplete cover. *Water Resour Res* 8: 1204–1213.
47. Allen RG, Pereira LS, Raes D, et al. (1998) FAO Irrigation and Drainage Paper 56. FAO, Rome, Italy.
48. Sloan PG, Moore ID (1984) Modeling subsurface storm flow on steeply sloping forested watersheds. *Water Resour Res* 20: 1915–1822.
49. Flanagan D C, Livingston SJ (1995) Water Erosion Prediction Project (WEPP) Version 95.7: User summary. NSERL Report No. 11. West Lafayette, Ind.: USDA-ARS National Soil Erosion Research Laboratory.
50. Kliewer WM, Wolpert JA, Benz M (2000) Trellis and vine spacing effects on growth, canopy microclimate, yield and fruit composition of cabernet sauvignon. In: *Acta Horticulturae* 526: 21–31
51. Stevens RM, Nicholas PR (1994) Root length and mass densities of Vitis vinifera L. cultivars "Muscat Gordo Blanco" and "Shiraz". *New Zeal J Crop Hortic Sci* 22: 381–385.
52. Alberts EE, Nearing MA, Weltz MA, et al. (1995) Soil component. In USDA Water Erosion Prediction Project: Hillslope Profile and Watershed Model Documentation. NSERL Report No. 2. D. C. Flanagan and M. A. Nearing, eds. West Lafayette, Ind.: USDA-ARS.
53. Flanagan DC, Nearing MA, eds (1995) USDA Water Erosion Prediction Project hillslope and watershed model documentation. NSERL Report No. 10. West Lafayette, Ind.: USDA-ARS National Soil Erosion Research Laboratory.
54. Moriasi DN, Arnold JG, Van Liew MW, et al. (2007) Model evaluation guidelines for systematic quantification of accuracy in watershed simulations. *Trans ASABE* 50: 885–900.
55. Nash JE, Sutcliffe JV (1970): River flow forecasting through conceptual models part I — A discussion of principles. *J Hydrol* 10: 282–290.
56. Gupta HV, Sorooshian S, Yapo PO (1999) Status of automatic calibration for hydrologic models: Comparison with multilevel expert calibration. *J Hydrolc Eng* 4: 135–143.
57. Ramos MC, Porta J (1997) Analysis of design criteria for vineyard terraces in the mediterranean area of North East Spain. *Soil Technol* 10: 155–166.
58. Verheijen FGA, Jones RJA, Rickson RJ, et al. (2009) Tolerable versus actual soil erosion rates in Europe. *Earth Sci Rev* 94: 23–38

59. Troeh FR, Hobbs JA, Donahue RL (1999) *Soil and Water Conservation: Productivity and Environmental Protection*, 3rd Edition. Prentice Hall. Upper Saddle River, New Jersey. 610 p
60. Mannering JV. The use of soil loss tolerances as a strategy for soil conservation. In: Editor, RPC Morgan. Soil Conservation Problems and Prospects; 1980 July 21st-25th; Silsoe, Beford, UK. Wiley.
61. Licciardello F, Taguas EV, Barbagallo S, et al. (2013) Application of the Water Erosion Prediction Project (WEPP) in Olive Orchards on Vertic Soil with Different Management Conditions. *Trans ASABE* 56: 951–961.
62. Routschek A, Schmidt J, Kreienkamp F (2014) Impact of climate change on soil erosion—A high-resolution projection on catchment scale until 2100 in Saxony/Germany. *Catena* 121: 99–109.
63. Ramos MC, Martínez-Casasnovas JA (2007) Soil loss and soil water content affected by land levelling in Penedès vineyards, NE Spain. *Catena* 71: 210–217.
64. Favis-Mortlock DT, Savabi MR (1996) Shifts in rates and spatial distributions of soil erosion and deposition under climate change. *Adv Hillslope Process* 1: 529-560
65. Nearing MA, Pruski FF, O'Neal MR (2004) Expected climate change impacts on soil erosion rates: A review. *J Soil Water Conserv* 59: 43–50.
66. Pruski FF, Nearing MA (2002) Climate-induced changes in erosion during the 21st century for eight U.S. locations. *Water Resour Res* 38: 341–3411.
67. García-Díaz A, Bienes R, Sastre B (2015) Study of Climatic Variations and its Influence on Erosive Processes in Recent Decades in One Location of Central Spain. *Engineering Geology for Society and Territory* - Volume 1: Climate Change and Engineering Geology, 105-108.
68. Shiono T, Ogawa S, Miyamoto T, et al. (2013) Expected impacts of climate change on rainfall erosivity of farmlands in Japan. *Ecol Eng* 61: 678–689.
69. Klik A, Konecny F (2013) Rainfall erosivity in northeastern Austria. *Trans ASABE* 56: 719–725.
70. Fiener P, Auerswald K, Winter F, et al. (2013) Statistical analysis and modelling of surface runoff from arable fields in central Europe. *Hydrol Earth Syst Sci* 17: 4121–4132.
71. Ramos MC, Benito C, Martínez-Casasnovas JA (2015) Simulating soil conservation measures to control soil and nutrient losses in a small, vineyard dominated basin. *Agric Ecosyst Environ* 213, 194-208.
72. Yang Q, Meng F-R, Zhao Z, et al. (2009) Assessing the impacts of flow diversion terraces on stream water and sediment yields at a watershed level using SWAT model. *Agric Ecosyst Environ* 132: 23–31.
73. Mwangi HM. Evaluation of the impacts of soil and water conservation practices on ecosystem services in Sasumua watershed, Kenya, using SWAT model. 2013. Available from: http://ir.jkuat.ac.ke/handle/123456789/994
74. Chow TL, Rees HW, Daigle JL (1999) Effectiveness of terraces/grassed waterway systems for soil and water conservation: A field evaluation. *J Soil Water Conserv* 54: 577–583.
75. Dumbrovský M, Sobotková V, Šarapatka B, et al. (2014) Cost-effectiveness evaluation of model design variants of broad-base terrace in soil erosion control. *Ecol Eng* 68: 260–269.

AIMS Press